Pedestrian motion modeled by FP-constrained Nash games

Souvik Roy, Alfio Borzì, Abderrahmane Habbal

Pedestrian motion modeled by FP-constrained Nash games

S. Roy*   A. Borzì†   A. Habbal‡

Abstract

A new approach to modeling pedestrian's avoidance dynamics based on a Fokker-Planck Nash game framework is presented. In this framework, two interacting pedestrian are considered, whose motion variability is modeled through the corresponding probability density functions (PDFs) governed by Fokker-Planck equations. Based on these equations, a Nash differential game is formulated where the game strategies represent controls aiming at avoidance by minimizing appropriate collision cost functionals. Existence of Nash equlibria solution is proved and characterized as solution to an optimal control problem that is solved numerically. Results of numerical experiments are presented that successfully compare the computed Nash equilibria to output of real experiments (conducted with humans) for 4 test cases.

- **Keywords:** pedestrian motion, avoidance, Fokker-Planck equation, differential games, Nash equilibrium, optimal control

- **MSC Classification:** 35Q84, 35Q91 35Q93, 49J20, 49K20, 65C20, 91A80, 91F99

1   Introduction

Crowd motion is a complex social and biological process [2, 3], involving psychological and nondeterministic behavioral decisions. It involves features like pattern formation, e.g. groups and lanes, and non-rational dynamics like as in a panic situation. A good knowledge of crowd (or pedestrian) flow scenarii is of utmost importance for urban management and safe evacuation [3], hence the importance of realistic modeling and simulation, notably with the help of mathematical and computational tools. There is a huge literature dedicated to the modeling of crowd motion, starting from original studies in the late '50 [15], and the early paper [11] where fluid mechanics models are proposed, and the paper [10] where pedestrian are modeled as interacting particles with mechanical attractive-repulsive forces. Presently, pedestrian modeling encompasses mathematical approaches ranging from discrete and cellular automata to continuum fluid dynamics and conservation laws; see, e.g., [2, 6, 9, 16, 19].

In this framework, *avoidance* is one of the most important features in pedestrian motion [7], involving non-cooperative and possibly non local interactions. Understanding the avoidance mechanisms has attracted many attention from experimentalists; see, e.g. [13, 18, 22]. However, despite the obvious relevance of a game-theoretic framework, to the best of our knowledge only a very few publications are dedicated to the investigation of this fundamental process. Let us mention [22] where human experiments are led to assess the interaction-based decision making involved in the

---

*Institut für Mathematik, Universität Würzburg, Emil-Fischer-Strasse 30, 97074 Würzburg, Germany. (souvik.roy@mathematik.uni-wuerzburg.de).

†Institut für Mathematik, Universität Würzburg, Emil-Fischer-Strasse 30, 97074 Würzburg, Germany. (alfio.borzi@mathematik.uni-wuerzburg.de)

‡Université Côte d'Azur, Inria, CNRS, LJAD, UMR 7351, Parc Valrose, 06108 Nice, France. (habbal@unice.fr).

avoidance behavior, and [12] where the modeling of deterministic pedestrian flow within an ODE optimal control and differential games framework is studied. There is also an important literature using the mean-field games approaches to model pedestrian motion, see for instance [14] and the references therein. These approaches do however basically assume a large number of agents or of interacting particles (refer to the note [4]).

In this paper, we introduce a new approach that starts from the framework developed in [20], where optimal control of crowd motion in the framework of stochastic processes and the related Fokker-Planck equations is discussed, and considers *two* individuals, who behave with rationality (in the game vocabulary sense) and have enough motion variability to be suitably described by the probability density functions -PDFs- of their motions. Specifically, the dynamics of the two pedestrian are assumed to be stochastic processes modeled by stochastic differential equations (SDEs), each with a drift composed of a desired velocity and a control function. Corresponding to these SDEs, the related Fokker-Planck (FP) equations are considered that model the evolution of the PDFs of the state (position) of the pedestrian. These FP equations are parabolic convection-diffusion equations where the convective coefficient corresponds to the drift of the SDE and thus inherits the control mechanism, which represent the players' strategy for avoidance. On the other hand, a main contribution of our work is the formulation of functional objectives that appropriately model the chance of collision that needs to be minimized by the action of the controls and subject to the differential constraints given by the FP equations of the two pedestrian. Our next essential step is the formulation of the avoidance problem as a static Nash game with complete information such that the avoidance dynamics arises as a Nash equilibrium of the game. We remark that in our framework, the concept of Nash equilibrium for modeling the decision-making control for collision avoidance plays a central role, and results in the formulation of a partial-differential game governed by FP equations where the control is included in the drift of the stochastic pedestrian motion and cost functionals for each pedestrian are defined that include a cost of the control and a collision-penalizing term. We prove existence of optimal Nash equilibria solutions and investigate regularity of these solutions. For the numerical solution of the proposed partial-differential games, an approximation and optimization framework for the fast computation of Nash solutions is discussed. The resulting FP-Nash computational framework for pedestrian motion is benchmarked with results of real experiments from cognitive psychology studies. An important feature of the present approach is that the pedestrian dynamics arise as a result -a Nash equilibrium- of interaction with prescribed rules, whilst in classical approaches the dynamics are prescribed. In other words, the present game approach explains *why* the observed dynamics arise, while classical phenomenological approaches, inspired e.g. from fluid dynamics (see [2, 6, 9, 19]) prescribe *how* the dynamics should be.

In the next section, we formulate our FP-Nash game model for avoidance. On the one hand, we motivate the modeling of the positions of pedestrian (the players) with stochastic differential models and with the corresponding FP equations. On the other hand, in the framework of differential games, we introduce into each SDE, and correspondingly FP, a control function that represents the strategy of the player with the purpose of optimizing its own objective. In Section 3, these objectives are formulated in terms of the PDFs of the state of the pedestrian and consist of a terminal observation term, a control cost and a collision functional. Further, the avoidance problem is defined as a Nash equilibrium problem and its solution is characterized as the minimum of a composite reduced cost functional. In Section 4, the solution of this composite minimization problem is framed as a control-constrained optimal control problem governed by the two FP equations corresponding to the two pedestrians. For this problem, we prove existence of an optimal solution and discuss its characterization as solution of a FP optimality system involving the two FP equations and the corresponding FP adjoint equations and optimality conditions. In Section 5, we carefully illustrate the setting and outcome of real experiments from cognitive psychology studies [13, 18, 22] that serve as

a benchmark for the results of our FP-Nash avoidance framework. Specifically, we consider 4 test cases where avoidance is observed with different dynamical and geometrical settings. For these test cases, we aim at reproducing a similar setting in our FP-Nash computational scheme and compare our results (trajectories) with those that have been recorded in the real experiments. The similarity between our results and the output of the real experiments with human behavior is impressive and supports the validity of our approach. A section of conclusion completes this work.

2   Formulation of the Nash game

Mathematical games may be static or dynamic. Roughly speaking, in a dynamic game, players sequentially observe others' actions and then choose their optimal responses. In a static game, players choose their best responses to the others without exchange (or communication) of information. Games may also be with complete information, meaning that all players know each others' strategy spaces and cost functionals (including their own ones). The failure of this assumption is termed as a game with incomplete information; see [8] for details.

We model our differential game *as static with complete information*. We consider $P \in \mathbb{N}$ players, $P \geq 2$, that evolve according to P stochastic differential equations (SDEs) driven by P time-dependent control functions. Specifically, the states of our players are denoted with $X^{(p)}$, $1 \leq p \leq P$, and belong to a space domain $\Omega \subset \mathbb{R}^D$ ($D \in \mathbb{N}^*$), which is assumed to be convex with Lipschitz boundary. We assume that the states of the players are subject to reflecting barriers, which may represent the walls of a room where the motion takes place. The time evolution of $X^{(p)}$ is governed by the following SDE

$$\begin{cases} dX^{(p)}(t) = b^{(p)}(X^{(p)}(t), t, u^{(p)}(t)) \, dt + \sigma \, dW(t) \\ X^{(p)}(0) = X_0^{(p)}, \end{cases} \tag{1}$$

where the drifts $b^{(p)}(X^{(p)}(t), t, u^{(p)}(t))$ have the structure

$$b^{(p)}(X^{(p)}(t), t, u^{(p)}(t)) = v^{(p)}(X^{(p)}(t), t) + u^{(p)}(t). \tag{2}$$

The velocity fields $v^{(p)}$ represent the deterministic dynamics of the single players in the absence of interaction with other players. This dynamics may represent the optimal (or preferred) path to satisfy the player's objective, e.g., to reach, with the shortest time, an arrival point A from a departure one D, where D and A belong to Ω.

The control functions $u^{(p)}$ represent the strategy that the players $X^{(p)}$ chose in order to satisfy the original objectives as much as possible taking into account the presence of the other players. In mathematical terms, the players' objectives can be formulated as follows

$$J_p(u^{(p)}, u^{(-p)}) = \alpha \mathbb{E}\left[V_p(X^p(T) - X_T^{(p)}) \right] + \frac{\nu}{2} \|u^{(p)}\|_{H^1(0,T)}^2 + W_p(X^{(p)}, X^{(-p)}), \tag{3}$$

where the potential V_p denotes a convex function of the state with minimum at $X_T^{(p)}$, which denotes the desired final state e.g., exit point) of the player p and the superscript $(-p)$ is used to emphasize the variables of player p and subsumes all the other players' variables. In (3), we also have a H^1 cost of the control, with weight $\nu > 0$, which guarantees a bounded control effort and a continuous slow-varying control. The term W_p is a key element of our work and it aims at modeling the interaction between players.

3

As shown in previous works [1, 20], a convenient framework that accommodates the minimization of (3) subject to the SDE constraints given by (1), originates from the observation that the entire statistics of the stochastic process, modeled by $X^{(p)}(t)$, is characterized by the probability density function (PDF) of this process. Moreover, if $f_0^{(p)}(x)$ represents the PDF of the initial state configuration $X_0^{(p)}$, then the evolution of the PDF $f^{(p)} = f^{(p)}(x, t)$ of the state $X^{(p)}$ at time t is governed by the following Fokker-Planck (FP) equation, $1 \le p \le P$,

$$\partial_t f^{(p)}(x,t) - \frac{\sigma^2}{2} \sum_{i,j=1}^n \partial^2_{x_i x_j} f^{(p)}(x,t) + \sum_{i=1}^n \partial_{x_i} \left(b_i^{(p)}(x,t,u_i^{(p)}(t)) f^{(p)}(x,t) \right) = 0, \tag{4}$$

$$f^{(p)}(x,0) = f_0^{(p)}(x) \tag{5}$$

This problem is considered in $Q = \Omega \times (0, T)$.

In this formulation, the initial vector PDF distribution satisfies the following conditions

$$f_0^{(p)} \ge 0, \qquad \int_\Omega f_0^{(p)}(x) dx = 1. \tag{6}$$

Corresponding to reflecting barriers for the stochastic model (1), we have flux zero boundary conditions for the FP equations. In order to formulate these boundary conditions, notice that the FP equations can be written in flux form as follows

$$\partial_t f^{(p)}(x,t) = \nabla \cdot F^{(p)}, \qquad f^{(p)}(x,0) = f_0^{(p)}(x), \tag{7}$$

where "$\nabla \cdot$" denotes the divergence operator and the flux $F^{(p)}$ is given component-wise by

$$F_j^{(p)}(x,t;f) = \frac{\sigma^2}{2} \partial_{x_j} f^{(p)} - b_j^{(p)}(x,t,u_j^{(p)}(t)) f^{(p)}.$$

Therefore flux-zero boundary conditions are formulated as follows

$$F^{(p)} \cdot n = 0, \qquad \text{on } \partial\Omega \times (0, T), \tag{8}$$

where n is the unit outward normal on $\partial\Omega$.

In [20], it is proved that for a given $u^{(p)} \in H^1(0, T)$, there exists a unique solution $f^{(p)} \in L^2(0, T; H^1(\Omega)) \cap C([0, T]; L^2(\Omega))$ to (4)-(8). Also in this reference it is proved that the control-to-state maps $u^{(p)} \mapsto f^{(p)}$ are differentiable.

In the FP framework, the players' objectives (3) can be reformulated as follows

$$\begin{aligned} J_p(u^{(p)}, u^{(-p)}) &= \alpha \int_\Omega V_p(x - x_T^{(p)}) f^{(p)}(x, T) dx + \frac{\nu}{2} \|u^{(p)}\|^2_{H^1(0,T)} \\ &+ W_p(f^{(p)}, f^{(-p)}). \end{aligned} \tag{9}$$

Notice that, since by the control-to-state map the PDF is a function of the control strategy, the PDF function does not appear as an argument of the objectives J_p, which is known as the reduced cost functional.

Our novel modeling step is the construction of the interaction functional $W_p(f^{(p)}, f^{(-p)})$. For this purpose and for clarity of our discussion, the remaining part of the paper is devoted to the case $P = 2$ of two pedestrian/players. However, our results can be extended to the more general case of $P > 2$.

4

Now, we start defining $W_p(f^{(1)}, f^{(2)})$ as a statistical expectation of the following general form :

$$W_p(f^{(1)}, f^{(2)}) = \int_0^T \mathbb{E}\Big\{ Q_p(t, X^{(1)}(t), X^{(2)}(t), u^{(1)}(X^{(1)}(t), t), u^{(2)}(X^{(2)}(t), t)) \Big\} dt \tag{10}$$

$$\text{or} \quad \max_{t \le T} \mathbb{E}\Big\{ Q_p(t, X^{(1)}(t), X^{(2)}(t), u^{(1)}(X^{(1)}(t), t), u^{(2)}(X^{(2)}(t), t)) \Big\}. \tag{11}$$

However, classical variants of this formulation are possible (like as considering the maximum of $\mathbb{E}(Q_p)$ over some prescribed schedules $t \in [t_i, t_{i+1}]$).

Regarding crowd behavior, apart from avoiding obstacles and seeking for optimal routes, we make the obvious assumption that two pedestrians would prefer to avoid being in the same space location at the same time.

Let us denote with $r > 0$ the overcrowding limit in the sense that the two pedestrians above would avoid a situation where $|X^{(2)}(t) - X^{(1)}(t)| < r$, where $|\cdot|$ denotes, e.g., the euclidean norm.

Thus, we may consider that the two players are aimed at minimizing the probability of such an event and we set $Prob\big\{|X^{(2)}(t) - X^{(1)}(t)| < r\big\} = \mathbb{E}(Q_p)$, where Q_p is the following characteristic function

$$Q_p(X^{(1)}(t), X^{(2)}(t)) = \mathbf{1}_{\{|X^{(2)}(t) - X^{(1)}(t)| < r\}}.$$

Thanks to the independence of the two stochastic processes, $X^{(1)}(t)$ and $X^{(2)}(t)$, and assuming that r is small enough, we have

$$\mathbb{E}(Q_p) = \int_\Omega \int_\Omega \mathbf{1}_{|y-x| < \rho} f^{(1)}(x, t) f^{(2)}(y, t) dx dy \tag{12}$$

$$= \int_\Omega f^{(1)}(x, t) \int_{B(x,\rho)} f^{(2)}(y, t) dy dx \approx r^D \int_\Omega f^{(1)}(x, t) f^{(2)}(x, t) dx, \tag{13}$$

where $B(x, r)$ denotes the open ball $|y - x| < r$ in $\mathbb{R}^D$. The Fubini and averaging operations are licit since $f^{(1)}(\cdot, t)$ and $f^{(2)}(\cdot, t)$ are smooth enough as being solutions to the FP equations (provided some assumptions, see Theorem 1 in [1]).

Motivated by (13), we choose the interaction cost $W_p(f^{(1)}, f^{(2)})$ as follows

$$W_p(f^{(1)}, f^{(2)}) = \rho \int_\Omega f^{(1)}(t, x) f^{(2)}(t, x) dx, \tag{14}$$

where the parameter ρ is defined as $\rho = Cr^D$, and $C \ge 0$ denotes the relative strength of the interaction, tuned to balance the weights of the other terms in the cost functionals J_p in (9). Since we consider a symmetric interaction for both players, we omit the index p in W_p in the following.

3 Nash Equilibrium

In this section, we formulate our differential game whose solution is sought as a Nash equilibrium. We discuss the characterization of this equilibrium solution and prove its existence.

We state our two pedestrian differential game as follows: The aim of the pedestrian 1 is to choose the strategy $u^{(1)}$ to minimize

$$J_1(u^{(1)}, u^{(2)}) = \alpha \int_\Omega V_1(x - x_T^{(1)}) f^{(1)}(x, T) dx + \frac{\nu}{2} \|u^{(1)}\|_{H^1(0,T)}^2$$
$$+ \rho \int_0^T \int_\Omega f^{(1)}(x, t) f^{(2)}(t, x) dx dt,$$

(G1)

while the pedestrian 2 aims at minimizing the following functional with the strategy $u^{(2)}$ as follows

$$J_2(u^{(1)}, u^{(2)}) = \alpha \int_\Omega V_2(x - x_T^{(2)}) f^{(2)}(x, T) dx + \frac{\nu}{2} \|u^{(2)}\|_{H^1(0,T)}^2$$
$$+ \rho \int_0^T \int_\Omega f^{(1)}(x, t) f^{(2)}(t, x) dx dt,$$

(G2)

where $f^{(p)}$, $p = 1, 2$, satisfy the Fokker-Planck problem (4)-(5). However, since both objectives depend on both strategies, we assume that the players decide to pursue a Nash equilibrium solution of this game.

Let $U^{(p)}$ be the space of admissible strategies, $u^{(p)} \in U^{(p)}$. Then a Nash equilibrium (NE) is defined as a pair of strategies $(\bar{u}^{(1)}, \bar{u}^{(2)}) \in U^{(1)} \times U^{(2)}$ such that the following holds

$$(\bar{u}^{(1)}, \bar{u}^{(2)}) = arg \min_{u^{(1)} \in U^{(1)}} J_1(u^{(1)}, \bar{u}^{(2)}) \tag{15}$$

$$= arg \min_{u^{(2)} \in U^{(2)}} J_2(\bar{u}^{(1)}, u^{(2)}) \tag{16}$$

Notice that our objectives are not convex and therefore we cannot apply the Nash theorem [?] to state existence of a Nash equilibrium. On the other hand, by exploiting the structure of our differential game, namely the weak coupling, we prove existence of a Nash equilibrium solution in the following way : first, we show that solutions to a specific control problem are Nash equilibria of our game. Then, in the next section, we prove existence of solutions to this optimal control problem.

Let us denote

$$G_p(u^{(p)}) = \alpha \int_\Omega V_p(x - x_T^{(p)}) f^{(p)}(x, T) dx + \frac{\nu}{2} \|u^{(p)}\|_{H^1(0,T)}^2.$$

With this notation, we have the following reduced objectives

$$J_p(u^{(1)}, u^{(2)}) = G_p(u^{(p)}) + W(u^{(1)}, u^{(2)}). \tag{17}$$

In fact, with our setting, we have a separable game of the following form

$$Player(1): \quad J_1(u^{(1)}, u^{(2)}) = G_1(u^{(1)}) + W(u^{(1)}, u^{(2)}),$$

(18)

$$Player(2): \quad J_2(u^{(1)}, u^{(2)}) = G_2(u^{(2)}) + W(u^{(1)}, u^{(2)}).$$

Notice that, if the pedestrians are not sensitive to overcrowding, that is if ρ is small enough, then the present game belongs to the family of weakly coupled games, and has a very useful separable structure. In the limit case where $\rho = 0$, there is no game taking place, and we get only two independent single decision-making control problems.

Now, we define the following composite cost functional

$$\hat{\mathcal{J}}(u^{(1)}, u^{(2)}) = G_1(u^{(1)}) + G_2(u^{(2)}) + W(u^{(1)}, u^{(2)}), \tag{19}$$

and consider the optimal control problem

$$\min \hat{\mathcal{J}}(u^{(1)}, u^{(2)}), \qquad (u^{(1)}, u^{(2)}) \in U^{(1)} \times U^{(2)}.$$

In the following theorem, we prove that the solution to this optimal control problem is a Nash equilibrium of our game.

Theorem 3.1. *Assume that $\hat{\mathcal{J}}$ has a minimum $\bar{u} = (\bar{u}^{(1)}, \bar{u}^{(2)})$. Then $(\bar{u}^{(1)}, \bar{u}^{(2)})$ is a Nash equilibrium of the game* (15)-(16).

Proof. For all $u^{(1)}, u^{(2)} \in U^{(1)} \times U^{(2)}$, we have $\hat{\mathcal{J}}(\bar{u}^{(1)}, \bar{u}^{(2)}) \leq \hat{\mathcal{J}}(u^{(1)}, u^{(2)})$, that is,

$$G_1(\bar{u}^{(1)}) + G_2(\bar{u}^{(2)}) + W(\bar{u}^{(1)}, \bar{u}^{(2)}) \leq G_1(u^{(1)}) + G_2(u^{(2)}) + W(u^{(1)}, u^{(2)}).$$

Now, set $u^{(1)} = \bar{u}^{(1)}$ to obtain :

$$G_2(\bar{u}^{(2)}) + W(\bar{u}^{(1)}, \bar{u}^{(2)}) \leq G_2(u^{(2)}) + W(\bar{u}^{(1)}, u^{(2)}), \qquad \forall u^{(2)} \in U^{(2)}.$$

This can be equivalently written as follows

$$J_2(\bar{u}^{(1)}, \bar{u}^{(2)}) \leq J_2(\bar{u}^{(1)}, u^{(2)}), \qquad \forall u^{(2)} \in U^{(1)}.$$

With the same reasoning, we also obtain

$$J_1(\bar{u}^{(1)}, \bar{u}^{(2)}) \leq J_1(u^{(1)}, \bar{u}^{(2)}), \qquad \forall u^{(1)} \in U^{(1)}.$$

Thus the claim is proved. □

This theorem states that the existence of a minimum of $\hat{\mathcal{J}}$ is a sufficient condition for a Nash equilibrium. On the other hand, this condition is not necessary, in the sense that there can be Nash equilibria that are not minima of $\hat{\mathcal{J}}$.

Notice that Theorem 3.1 is the starting point to apply tools from computational optimization to compute this equilibrium. This is the two-fold purpose of the next section.

4   An optimal control problem

We recall that our Nash equilibrium $\bar{u} = (\bar{u}^{(1)}, \bar{u}^{(2)})$ satisfies the optimal control problem :

$$\hat{\mathcal{J}}(\bar{u}) \leq \hat{\mathcal{J}}(u) \qquad \text{for all } u = (u^{(1)}, u^{(2)}) \in U^{(1)} \times U^{(2)},$$

which is the formulation of our optimization problem in reduced form. Thus, by explicitly stating the dependence of the PDFs on the control strategies, our optimization problem is explicitly given by

$$\min \hat{\mathcal{J}}(f^{(1)}, f^{(2)}, u^{(1)}, u^{(2)}) := G_1(f^{(1)}, u^{(1)}) + G_2(f^{(2)}, u^{(2)}) + W(f^{(1)}, f^{(2)}) \tag{20}$$

$$\partial_t f^{(1)}(x,t) - \frac{\sigma^2}{2} \sum_{i,j=1}^{n} \partial^2_{x_i x_j} f^{(1)}(x,t) + \sum_{i=1}^{n} \partial_{x_i}\left(b_i^{(1)}(x,t,u_i^{(1)}(t)) f^{(1)}(x,t)\right) = 0, \tag{21}$$

$$f^{(1)}(x,0) = f_0^{(1)}(x), \tag{22}$$

$$\partial_t f^{(2)}(x,t) - \frac{\sigma^2}{2} \sum_{i,j=1}^{n} \partial^2_{x_i x_j} f^{(2)}(x,t) + \sum_{i=1}^{n} \partial_{x_i}\left(b_i^{(2)}(x,t,u_i^{(2)}(t)) f^{(2)}(x,t)\right) = 0, \tag{23}$$

$$f^{(2)}(x,0) = f_0^{(2)}(x), \tag{24}$$

where we require that the strategies $u^{(p)} = (u_1^{(p)}, \ldots, u_n^{(p)})$, $p = 1, 2$, are in the following admissible set

$$U^{(p)} = \{u \in H_0^1(0,T) | \ u_a \le u_i(t) \le u_b, \ i = 1, \ldots, n \text{ a.e. in } (0,T)\} \tag{25}$$

where $u_a, u_b \in \mathbb{R}$, $u_a < u_b$.

Next, we discuss the existence of solutions to the optimal control problem (20) - (25). For this purpose, in the following proposition, we address the properties of the cost functional $\hat{\mathcal{J}}$.

Proposition 4.1. *The objective functional* (20) *is sequentially weakly lower semicontinuous (w.l.s.c.), bounded from below, coercive on $U^{(1)} \times U^{(2)}$, and it is Fréchet differentiable.*

The proof of this proposition is straightforward, once one recalls that the PDFs are nonnegative functions.

The next result states existence of an optimal control $\bar{u}$.

Proposition 4.2. *Assume that $f_0 = (f_0^{(1)}, f_0^{(2)}) \in H^1(\Omega) \times H^1(\Omega)$ and $f_0^{(p)}$ satisfies* (6), *and the objective is given by* (20). *Then there exists $\bar{f} = (\bar{f}^{(1)}, \bar{f}^{(2)}) \in C([0,T]; H^1(\Omega; \mathbb{R}^2)) \times C([0,T]; H^1(\Omega; \mathbb{R}^2))$ and $\bar{u} = (\bar{u}^{(1)}, \bar{u}^{(2)}) \in U^{(1)} \times U^{(2)}$ such that $\bar{f}$ solves the FP constraints (21)-(24) and $\bar{u}$ minimizes $\hat{\mathcal{J}}$ in $U^{(1)} \times U^{(2)}$.*

Proof. Boundedness from below of $\hat{\mathcal{J}}$ guarantees the existence of a minimizing sequence $(u^m) \in U^{(1)} \times U^{(2)}$. Since $U^{(1)} \times U^{(2)}$ is reflexive and $\hat{\mathcal{J}}$ is sequentially w.l.s.c. and coercive in $H_0^1(0,T) \times H_0^1(0,T)$, this sequence is bounded. Therefore it contains a weakly convergent subsequence (u^{m_l}) such that $u^{m_l} \rightharpoonup \bar{u}$. Moreover since the embedding $H^1(0,T) \subset\subset C(0,T)$ is compact, we have strong convergence $u^{m_l} \to \bar{u}$ in $C([0,T]; \mathbb{R}^2)$.

In correspondence of the sequence (u^{m_l}), the solution of the FP equations results in the bounded sequence $(f^{m_l}) \in [L^2(0,T; H^1(\Omega)) \cap C([0,T]; L^2(\Omega))]^2$ while the sequence of the time derivatives, $(\partial_t f^{m_l})$, is bounded in $[L^2(0,T; H^{-1}(\Omega))]^2$. Therefore both sequences converge weakly to $\bar{f}$ and $\partial_t \bar{f}$, respectively. Further, by the Theorem of Aubin-Lions [?], we have that there exists a subsequence of (f^{m_l}), which we denote with the same index, that converges strongly in $[L^2(0,T; L^2(\Omega; \mathbb{R}^2))]^2$.

Concerning the terms $\nabla \cdot (b,x,t,u)f)$, recall the structure of b given in (2) and the fact that u is only time dependent. Therefore the sequence of the products $b(\cdot,\cdot,u^{m_l})f^{m_l}$ converges strongly in $[L^2(0,T; L^2(\Omega; \mathbb{R}^2))]^2$. Finally, considering these limiting sequences in the weak formulation of the FP problems, it follows that $\bar{f}$ corresponds to the solution of (21)-(24) with the control given by $\bar{u}$. Thus the pair $(\bar{f}, \bar{u})$ minimizes the cost functional $\hat{\mathcal{J}}$.

$\square$

Proposition 4.2 states existence of a local optimal solution. However, the presence of possible symmetries in the formulation of the game, like invariance under exchange of players or geometrical symmetries, suggest that multiple Nash equilibria must exist.

A local minimum $\bar{u}$ of $\hat{\mathcal{J}}$ is characterized by the first-order necessary optimality conditions given by $\langle \nabla \hat{\mathcal{J}}(\bar{u}), v - \bar{u} \rangle \geq 0$ for all $v \in U_{ad}$. We denote with $\langle \cdot, \cdot \rangle$ the $L^2(0, T; \mathbb{R}^n) \times L^2(0, T; \mathbb{R}^n)$ inner product (unless otherwise specified), and $\nabla \hat{\mathcal{J}}(\bar{u})$ denotes the $L^2(0, T; \mathbb{R}^n) \times L^2(0, T; \mathbb{R}^n)$ gradient as the Riesz representative, in the $L^2(0, T; \mathbb{R}^n) \times L^2(0, T; \mathbb{R}^n)$ Hilbert space, of the derivative functional $d\hat{\mathcal{J}}(\bar{u})$ evaluated at $\bar{u}$. We have $d\hat{\mathcal{J}}(\bar{u}) \cdot v = \langle \nabla \hat{\mathcal{J}}(\bar{u}), v \rangle$.

It is well known [5, 17, 21] that, in the framework of the adjoint method, the condition $\langle \nabla \hat{\mathcal{J}}(\bar{u}), v - \bar{u} \rangle \geq 0$ results in the following optimality system, consisting of forward- and backward FP problems and a variational inequality. We have

$$\partial_t f^{(1)}(x,t) - \frac{\sigma^2}{2} \sum_{i,j=1}^n \partial^2_{x_i x_j} f^{(1)}(x,t) + \sum_{i=1}^n \partial_{x_i} \left(b_i^{(1)}(x,t,u_i^{(1)}(t)) f^{(1)}(x,t) \right) = 0, \tag{26}$$

$$f^{(1)}(x,0) = f_0^{(1)}(x), \tag{27}$$

$$\partial_t f^{(2)}(x,t) - \frac{\sigma^2}{2} \sum_{i,j=1}^n \partial^2_{x_i x_j} f^{(2)}(x,t) + \sum_{i=1}^n \partial_{x_i} \left(b_i^{(2)}(x,t,u_i^{(2)}(t)) f^{(2)}(x,t) \right) = 0, \tag{28}$$

$$f^{(2)}(x,0) = f_0^{(2)}(x). \tag{29}$$

$$\begin{aligned} -\partial_t p^{(1)}(x,t) - \frac{\sigma^2}{2} \sum_{i=1}^n \partial^2_{x_i x_i} p^{(1)}(x,t) \quad &- \quad \sum_{i=1}^n b_i^{(1)}(x,t,u_i^{(1)}(t)) \partial_{x_i} p^{(1)}(x,t) \\ &+ \quad \rho f^{(2)}(x,t) = 0, \end{aligned} \tag{30}$$

$$p^{(1)}(x,T) = -\alpha V(x - x_T^{(1)}), \tag{31}$$

$$\begin{aligned} -\partial_t p^{(2)}(x,t) - \frac{\sigma^2}{2} \sum_{i=1}^n \partial^2_{x_i x_i} p^{(2)}(x,t) \quad &- \quad \sum_{i=1}^n b_i^{(2)}(x,t,u_i^{(1)}(t)) \partial_{x_i} p^{(2)}(x,t) \\ &+ \quad \rho f^{(1)}(x,t) = 0, \end{aligned} \tag{32}$$

$$p^{(2)}(x,T) = -\alpha V(x - x_T^{(2)}). \tag{33}$$

Further, the optimality condition is given by

$$\left(\nu u_k^{(p)} - \nu \frac{\partial^2 u_k^{(p)}}{\partial t^2} - \int_\Omega \frac{\partial p^{(p)}}{\partial x_k} f^{(p)} dx, v_k^{(p)} - u_k^{(p)} \right)_{L^2(0,T)} \geq 0 \qquad \forall v_k^{(p)}, \ k = 1, \dots, n, \tag{34}$$

where $v_k^{(p)}$ represents the k-th component of $v^{(p)} \in U_p$; here, $\langle \cdot, \cdot \rangle$ represents the $L^2(0,T)$ inner product.

Notice that in the optimality system, the following reduced L^2 gradient components appear

$$\nabla_{u_k}\hat{\mathcal{J}}(u) = \nu u_k - \nu \frac{\partial^2 u_k^{(p)}}{\partial t^2} - \int_\Omega \frac{\partial p}{\partial x_k} f \, dx, \qquad k = 1, \ldots, n. \tag{35}$$

Here and below, the Laplacian is meant in the weak sense, and assuming that the last term in (35) is in $H^{-1}(0, T)$, then the solution of the gradient equation with homogeneous Dirichlet boundary conditions results in $u \in H_0^1(0, T)$.

We wish to apply a gradient-based optimization scheme where the residual of (35) is used. For this purpose, we cannot use this residual directly for updating the control, since it is in $H^{-1}(0, T)$. Therefore, it is necessary to determine the reduced $H^1(0, T)$ gradient. This is done based on the following fact

$$\langle \nabla \hat{\mathcal{J}}(u)_{H^1}, \varphi \rangle_{H^1((0,T);\mathbb{R}^n)} = \langle \nabla \hat{\mathcal{J}}(u), \varphi \rangle_{L^2((0,T);\mathbb{R}^n)} \text{ for all } \varphi \in H^1((0, T); \mathbb{R}^n).$$

Using the definition of the H^1 inner product and integrating by parts, we have that the H^1 gradient is obtained by solving the following boundary value problem

$$-\Delta(\nabla_{u_k}\hat{\mathcal{J}}(u)_{H^1}) + (\nabla_{u_k}\hat{\mathcal{J}}(u)_{H^1}) = \nabla_{u_k}\hat{\mathcal{J}}(u) \qquad \text{in } (0, T), \tag{36}$$

$$(\nabla_{u_k}\hat{\mathcal{J}}(u)_{H^1}) = 0 \qquad \text{on } \partial(0, T), \tag{37}$$

where $k = 1, \ldots, n$, and Δ denotes the Laplace operator in time.

The solution to this problem provides the appropriate gradient to be used in a gradient update of the control that includes projection to satisfy the given control constraints.

5   Numerical experiments

In this section, we consider 4 different test cases to discuss the efficiency and robustness of our optimization setup for determining the Nash equilibrium pair $(\bar{u}^{(1)}, \bar{u}^{(2)})$ for the differential game (15)-(16). To assess the ability of our approach to model avoidance dynamics, we compare our results to real human experiments from the cognitive psychology studies in [13, 18, 22].

The motion of the players are represented by the motion of their PDF's. In the plots, the trajectories of the players depict the trajectories of the mean of their respective PDF's. The initial density for the players are defined as

$$f_0(x) = \hat{C} e^{-\{(x_1-A_1)^2-(x_2-A_2)^2\}/0.5}, \tag{38}$$

where $(A_1, A_2) = x_t(0)$ is the starting point of the players x_t, $\hat{C}$ is a normalization constant such that

$$\int_\Omega f_0(x) dx = 1$$

and $x = (x_1, x_2)$. The terminal potential for both the players are defined as

$$V(x - x_T^{(p)}) = (x - x_T^{(p)})^2, \; p = 1, 2,$$

where $x_T^{(p)}$ is the terminal position of the two players. The parameter α is set to be 100 and $\nu = 1$.

10

The differential game constitutes of determining Nash equilibrium strategies $(u_{NE}^{(1)}, u_{NE}^{(2)})$ for the players A and B, respectively such that they avoid interaction with each other while maintaining their respective drifts in order to reach the terminal point. The intensity of avoidance is dependent on the factor ρ.

We solve the optimal control problem (20) - (25), which yields a Nash equilibrium, using a gradient-based optimization scheme exactly as in [20].

In the following, we use the notations $D^{(p)}$ and $A^{(p)}$ to define respectively (D)eparture and (A)rrival locations of players A for $p = 1$, and B for $p = 2$.

5.1 Test-case I: Huber-135

The test-case Huber-135 corresponds to the experiment in [13] where trajectories of agents A and B form an angle of $135°$. The computational setting is the following: we consider the motion of A and B in a square domain $\Omega = [-3, 3] \times [-3, 3]$ for a time interval $[0, 3]$. Player A starts its motion from the departure point $D^{(1)} = (-1, 0)$ and player B starts its motion from the point $D^{(2)} = (1, 1)$. The drift $v^{(1)}$ for player A is $(1, 0)$, thus it moves along x-axis. The drift $v^{(2)}$ for player B is $(-1, -1)$ and thus, it moves down diagonally. The arrival position of player A is $A^{(1)} = (2, 0)$ and for player B is $A^{(2)} = (-2, -2)$. The spatial and the temporal domains are divided into 50 uniformly distributed subintervals. The settings for the game is shown in Figure 1.

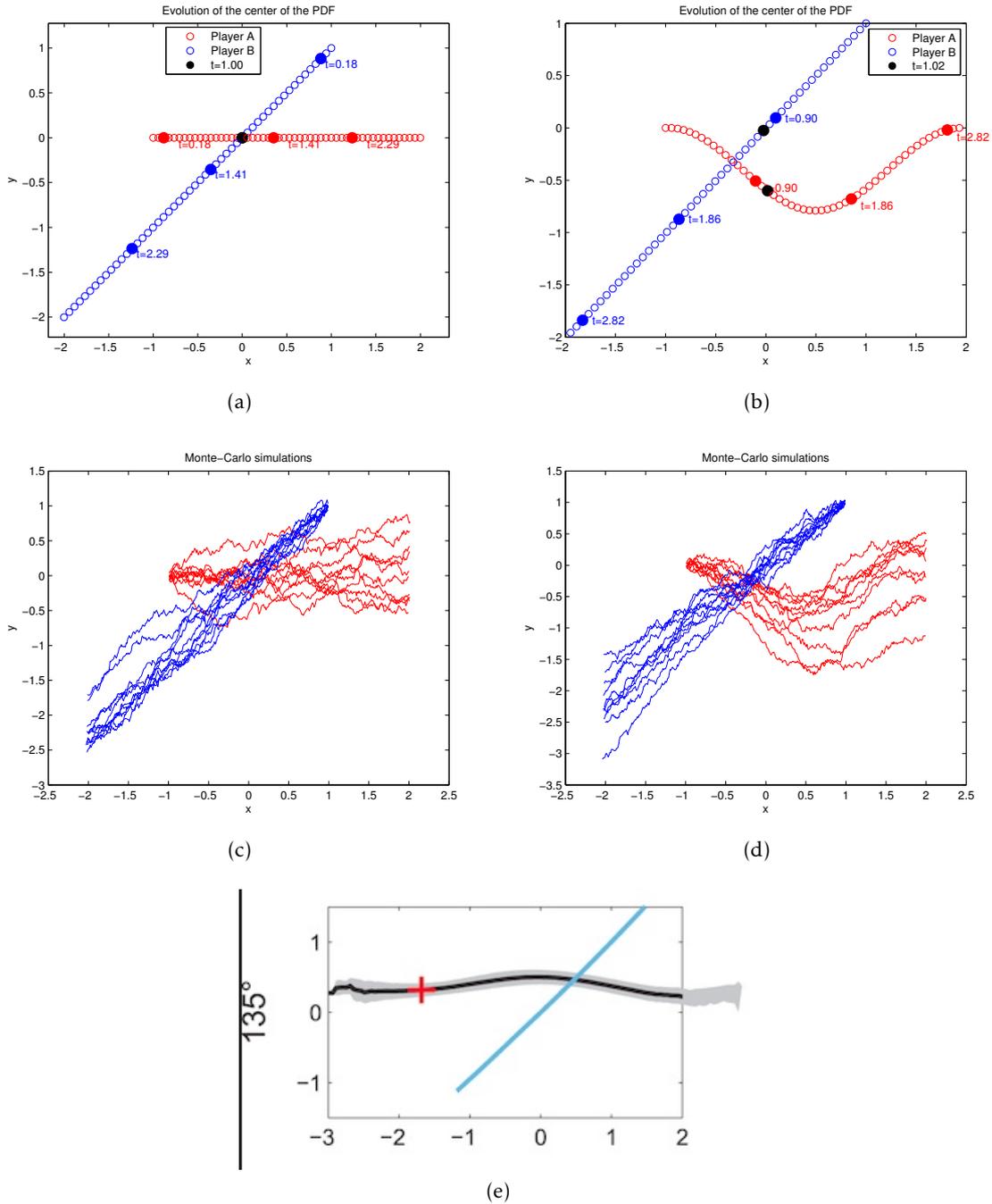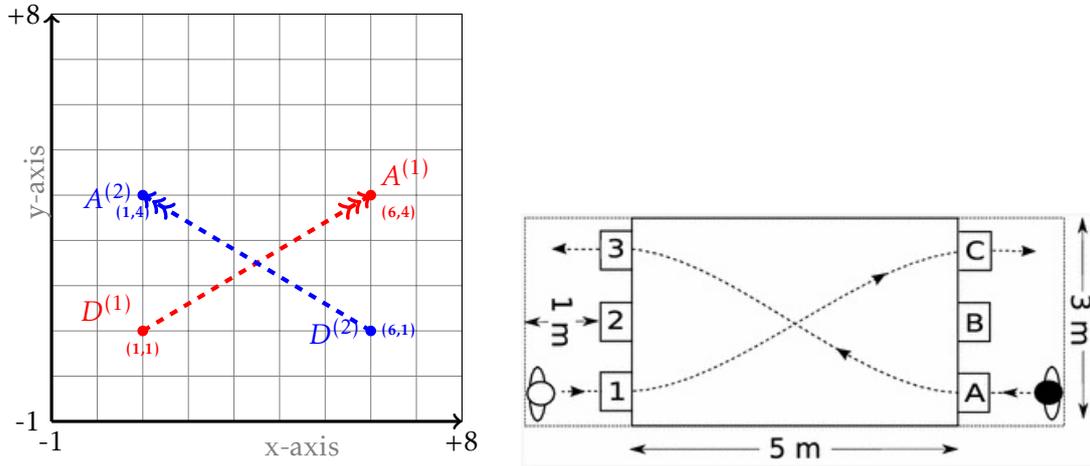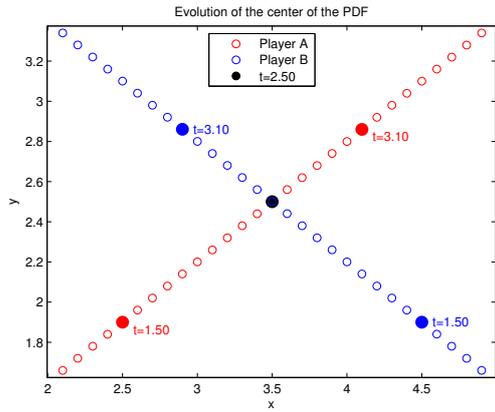Figure 1: Settings for the game described in test-case Huber-135

(a)

(b)

(c)

(d)

(e)

Figure 2: Case 1: Figures 2a and 2b show the plots of the mean of the PDFs for $\rho = 0.01, 200$ respectively.Figures 2c and 2d show the Monte-Carlo simulations for $\rho = 0.01, 200$ respectively. Figure 2e shows the results of the corresponding human experiment from [13].

Figures 2a and 2b show the plots of the mean of the PDFs for $\rho = 0.01, 200$ respectively. We can see that for $\rho = 0.01$, the two players meet at time $t = 1.0$ as denoted by the black dot. In the case of $\rho = 200$, player A goes around player B to avoid intersection as is shown from the position of the players at time $t = 1.0$ with the black dot. Figures 2c and 2d show the Monte-Carlo simulations for $\rho = 0.01, 200$ respectively. Moreover, in both the cases we see that the two players reach their

final target ultimately. This is comparable to the results of the corresponding human experiment performed as in [13], which is shown in Figure 2e. However, there was no game involved in [13] as one of the experiment participants was a non-reactive interferer. We remark that in the present test-case, player B acts precisely as a non-reactive agent in the Nash equilibrium.

5.2   Test-case II: Turnwald 1C-A3

In the next test case, we consider an experiment from [22]. Two participants A and B are asked to walk from given initial to final points, the latter information being known to both players. In the present case, 1C-A3 means player A goes from "1 to C", and player B goes from "A to 3" as shown in Figure 3 (right). In our computational setting, the motion of A and B is in a square domain $\Omega = [-1,8] \times [-1,8]$ for a time interval $[0,5]$. Player A starts its motion from the departure point $D^{(1)} = (1,1)$ and player B starts its motion from the point $D^{(2)} = (6,1)$. The arrival position of player A is $A^{(1)} = (6,4)$ and for player B is $A^{(2)} = (1,4)$. The spatial and the temporal domains are divided into 50 uniformly distributed subintervals. The settings for the game is shown in Figure 3.
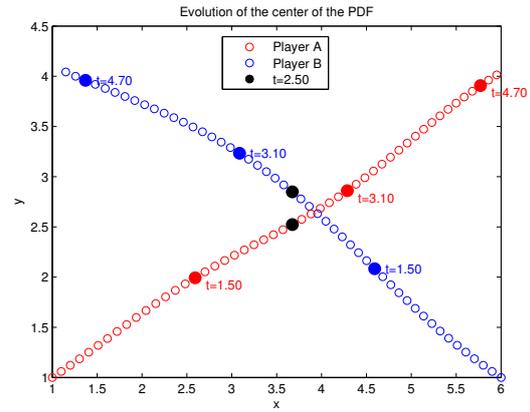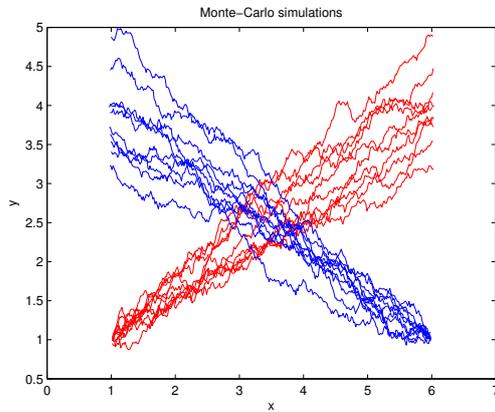

Figure 3: Settings for the Turnwald game described in test-case Turnwald 1C-A3: (left) the computational setting ; (right) the human experiment setting excerpt from [22].
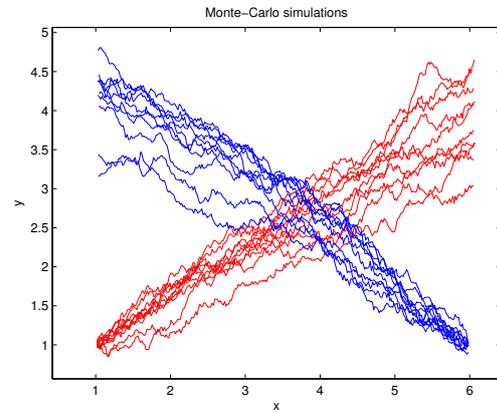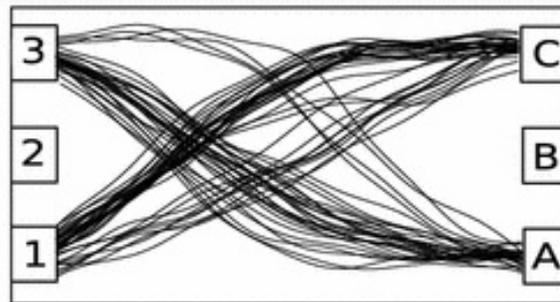
(a)

(b)

(c)

(d)

(e)

Figure 4: Case 3: Figures 4a and 4b show the zoomed-in plots of the mean of the PDFs for $\rho = 0.01, 200$ respectively. Left: Motion for $\rho = 0.01$. Figures 4c and 4d show the Monte-Carlo simulations for $\rho = 0.01, 200$ respectively. Figure 4e shows the Monte-Carlo simulations for the experimental results in [22].

Figures 4a and 4b show the zoomed-in plots of the mean of the PDFs for $\rho = 0.01, 200$ respectively. We notice that for $\rho = 0.01$, the two players meet at time $t = 2.5$ as denoted by the black dot. In the case of $\rho = 200$, players A and B move around each other to avoid intersection as is shown by their positions at time $t = 2.5$ with a black dot. Figures 4c and 4d show the Monte-Carlo simulations

14

for $\rho = 0.01, 200$ respectively. For $\rho = 200$, we see that, around the region where trajectories cross, the layout of the Monte-Carlo simulations is comparable with the one from [22] shown in Figure 4e. Notice that in Figure 4e, trajectories show features (slopes) different from those of Figure 4d. In our opinion, this is due to the fact that thanks to availability of visual information, the players can and indeed play a dynamic game, not a static one, and adapt their strategies by integrating the observed visual information.

5.3   Test-case III: Turnwald 1C-B2

In the next test case, we consider another experiment from [22]. In this case, player A goes from "B to 2" and player B goes from "1 to C" as shown in Figure 6e. In the computational setting shown in Figure 5, the motion of A and B is in the domain $\Omega = [-1, 1] \times [-3, 3]$ for a time interval $[0, 5]$. Player A starts its motion from the departure point $D^{(1)} = (0, -2.5)$ and player B starts its motion from the point $D^{(2)} = (-0.5, 2.5)$. The terminal position of player A is $A^{(1)} = (0, 2.5)$ and for player B is $A^{(2)} = (0.5, -2.5)$. The spatial and the temporal domains are divided into 50 uniformly distributed subintervals.
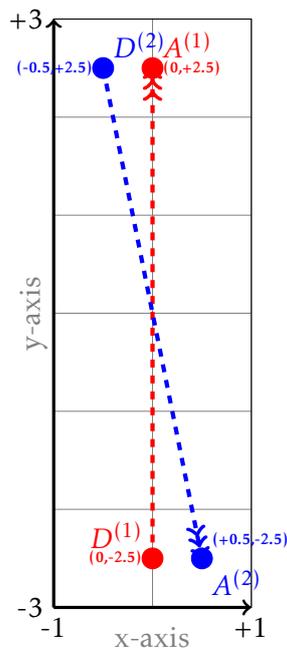

Figure 5: Settings for the Turnwald game described in test-case Turnwald 1C-B2
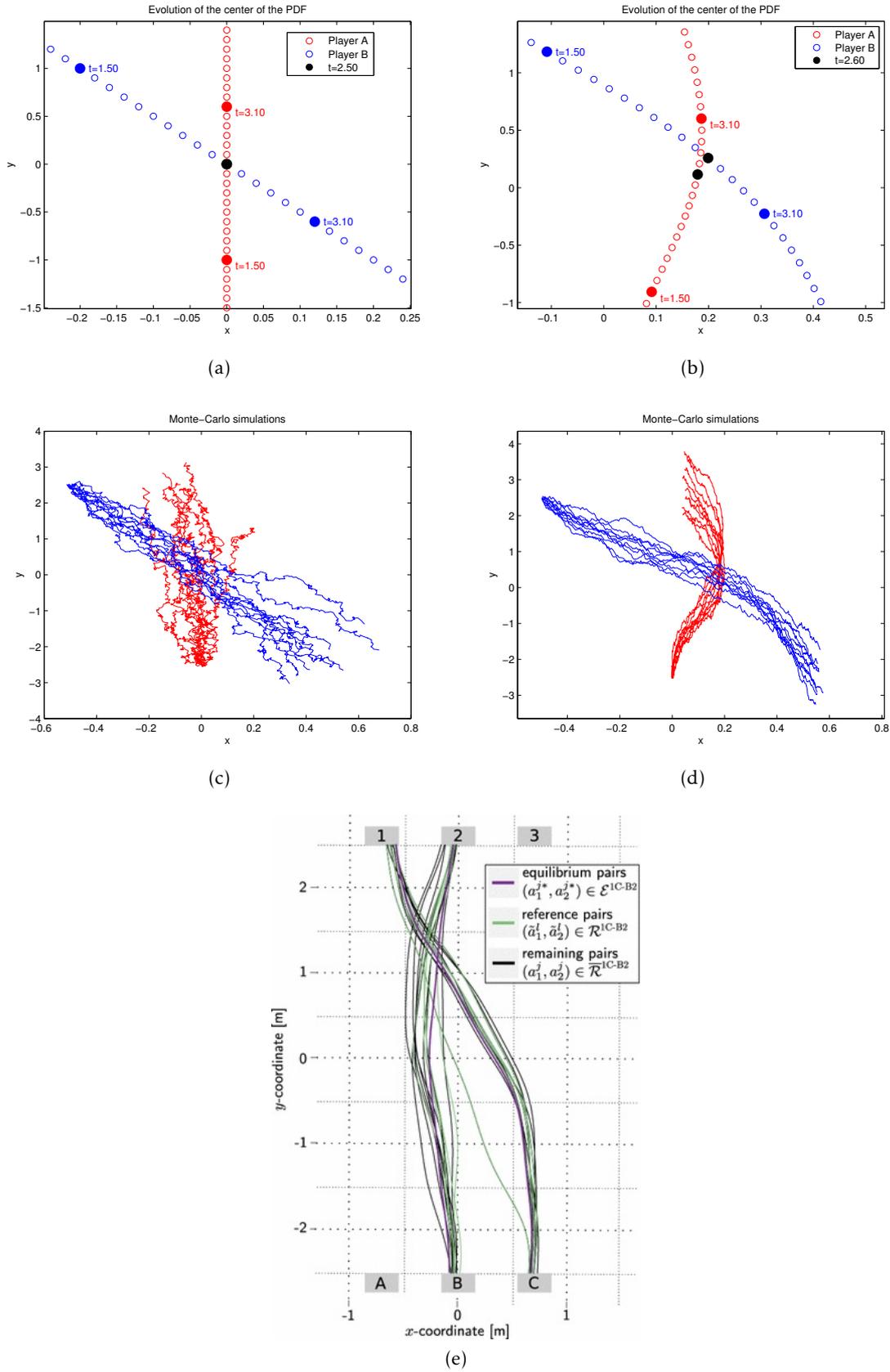
(a)

(b)

(c)

(d)

(e)

Figure 6: Case 4: Figures 6a and 6b show the zoomed-in plots of the mean of the PDFs for $\rho = 0.01, 150$ respectively. Left: Motion for $\rho = 0.01$. Figures 6c and 6d show the Monte-Carlo simulations for $\rho = 0.01, 150$ respectively. Figure 6e shows the Monte-Carlo simulations for the experimental results in [22].

Figures 6a and 6b show the zoomed-in plots of the mean of the PDFs for $\rho = 0.01, 150$ respectively. We notice that for $\rho = 0.01$, the two players meet at time $t = 2.5$ as denoted by the black dot. In the case of $\rho = 150$, players A and B move around each other to avoid intersection as is shown by their positions at time $t = 2.6$ with a black dot. Figures 6c and 6d show the Monte-Carlo simulations for $\rho = 0.01, 150$ respectively.

With respect to the previous experiment Turnwald 1C-A3, we see that for $\rho = 150$, the Monte-Carlo simulations show even more geometric similarities with the ones resulting from the human experiments in [22] as shown in Figure 6e. However, as in the previous test-case, we observe that our NE trajectories still exhibit differences with respect to the human experiment. This is due, in our opinion, to the same reasons discussed for Turnwald 1C-A3. Indeed, the participants play a dynamic game, and adapt their strategies according to the available visual information they get dynamically from the others.

For instance, for the two Turnwald human experiments, one of the players observes that the other player initiates a straight motion then reacts by deviating from straight line, following a path which ensures sufficiently large minimal predicted distance "MPD" as suggested in [18], but then by increasing the cost of the strategy. In our Nash game, the control over the cost of the strategies forces the trajectories of the players to deviate less, yielding a smaller MPD.

5.4 Test-case IV: Gait and Posture

In the final test case, we consider an experiment from [18] which we address as "Gait and Posture" experiment. In this experiment, two participants, separated by blankets, are asked to move across the experimental area, to reach a prescribed location, see Figure 7 (right). In our computational setting shown in Figure 7 (left), the motion of two players A and B is in a square domain $\Omega = [-10, 10] \times [-10, 10]$ for a time interval $[0, 1]$. Player A starts its motion from the departure point $D^{(1)} = (-7.5, -7.5)$ and player B starts its motion from the point $D^{(2)} = (-7.5, 7.5)$. The terminal position of player A is $A^{(1)} = (7.5, 7.5)$ and for player B is $A^{(2)} = (7.5, -7.5)$. The spatial and the temporal domains are divided into 50 uniformly distributed subintervals.
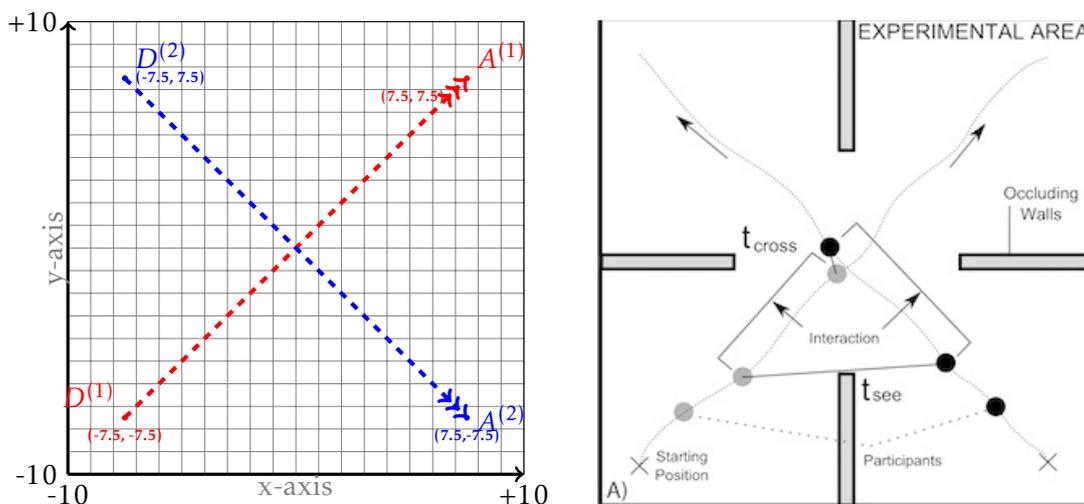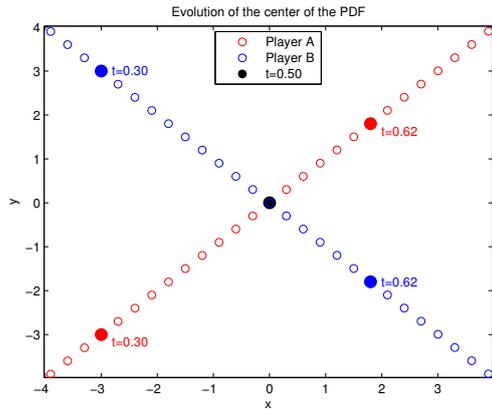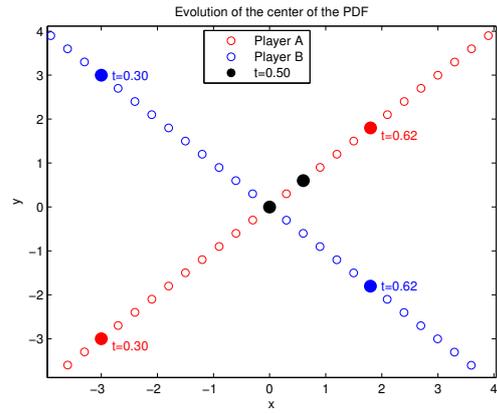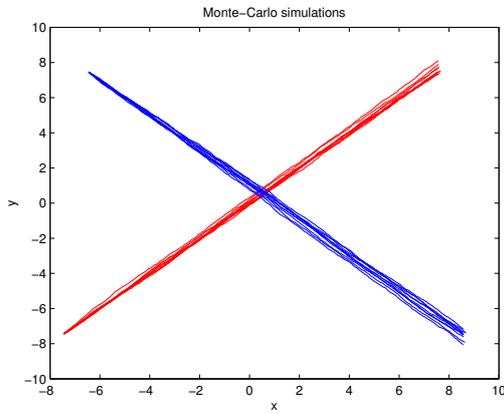

Figure 7: Computational (left) and experimental (right) settings for the Gait and Posture game described in test-case Gait and Posture
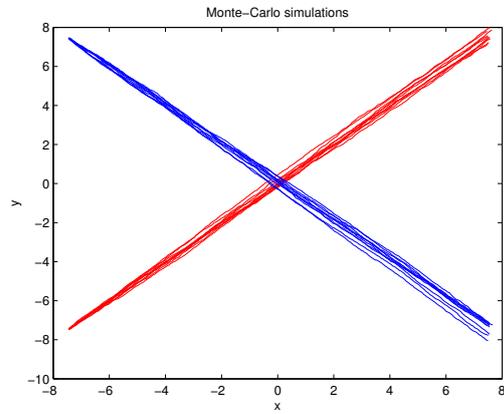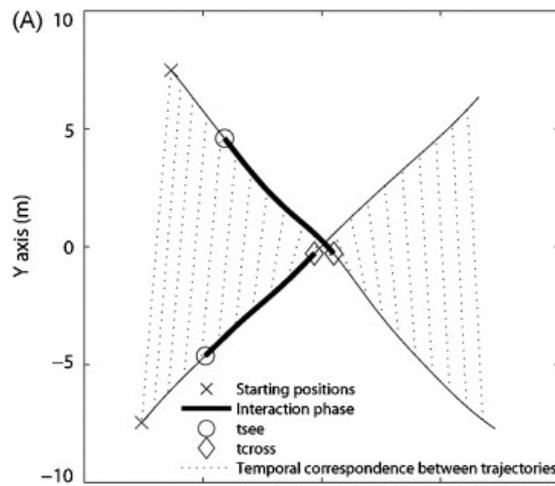
Figure 8: Case 2: Figures 8a and 8b show the zoomed-in plots of the mean of the PDFs for $\rho = 0.01, 200$ respectively. Figures 8c and 8d show the Monte-Carlo simulations for $\rho = 0.01, 200$ respectively. Figure 8e represents the trajectories for the experimental results in [18].

Figures 8a and 8b show the zoomed-in plots of the mean of the PDFs for $\rho = 0.01, 200$ respectively. We notice that for $\rho = 0.01$, the two players meet at time $t = 0.5$ as denoted by the black dot. In the case of $\rho = 200$, player A moves faster near the time of intersection $t = 0.5$ to avoid intersection with player B. After avoiding intersection, player A goes slower to reach its terminal target.

We remark that Figures 8b and 8e are in very good accordance with respect to the trajectories followed by both players as well as with respect to the velocity profiles. By observing the "temporal correspondence between trajectories" as in Figure 8e, we notice that one player moves faster near the time of intersection "tcross" to avoid intersection with other player. After avoiding intersection, the first player goes slower to reach its terminal target. In comparison to the previous Turnwald experiments, which involved early visual information weakening the static game assumption, here the human experiment is set up as a static (or blind or simultaneous) Nash game and the results of our computational model are strikingly similar to the results of the real human experiment.

6   Conclusion

A new approach to modeling pedestrian's avoidance dynamics based on a Fokker-Planck Nash game framework was presented and investigated theoretically and numerically. This approach attempts to explain why the observed dynamics arise, while classical phenomenological approaches prescribe how the dynamics should be. Based on Fokker-Planck equations, a Nash differential game was formulated where the game strategies represent controls aiming at avoidance by minimizing appropriate collision cost functionals. Existence of Nash equilibria solution was proved and characterized as solution to an optimal control problem. The resulting FP-Nash computational strategy for pedestrian motion was successfully benchmarked with results of real experiments from cognitive psychology studies. The proposed FP-Nash approach represents a powerful new paradigm for the theoretical investigation and computational simulation of differential games with non-convex cost functionals. It provides a very rich framework to model a large class of processes involved in pedestrian motion.

References

[1] M. Annunziato and A. Borzì. *A Fokker-Planck control framework for multidimensional stochastic processes*, Journal of Computational and Applied Mathematics, 237:487-507, 2013.

[2] N. Bellomo , A. Bellouquid, D. Knopoff. *From the micro-scale to collective crowd dynamics.* Multiscale Model. Simul, 11:943–963, 2013.

[3] N. Bellomo, D. Clarke, L. Gibelli, P. Townsend and B. J. Vreugdenhil. *Human behaviours in evacuation crowd dynamics: From modelling to big data toward crisis management.* Physics of Life Reviews, 18:55-65, 2016.

[4] A. Borzì and Marco Caponigro. *A control theoretical approach to crowd management: Comment on Human behaviours in evacuation crowd dynamics: From modelling to big data toward crisis management by Nicola Bellomo et al.*, Physics of Life Reviews, Volume 18, September 2016, Pages 27-28, ISSN 1571-0645, http://dx.doi.org/10.1016/j.plrev.2016.08.013.

[5] A. Borzì and V. Schulz. *Computational optimization of systems governed by partial differential equations*, SIAM book series on Computational Science and Engineering 08, SIAM, Philadelphia, PA, 2012.

[6] R. M. Colombo, P. Goatin, G. Maternini & M. D. Rosini. *Macroscopic Models for Pedestrian Flows.* in Big events and transport: the transportation requirements for the management of large scale events. 2010.

[7] A. Festa and M–T. Wolfram. *Collision avoidance in pedestrian dynamics.* Decision and Control (CDC), 2015 IEEE 54th Annual Conference on. IEEE, 2015.

[8] R. Gibbons. *A primer in game theory*, Harvester Wheatsheaf, 1992.

[9] P. Goatin and M. Mimault. *A mixed system modeling two-directional pedestrian flows.* Mathematical biosciences and engineering, 12(2):375-392, 2015.

[10] D. Helbing. *A mathematical model for the behavior of pedestrians.* Behavioral science, 36(4):298-310, 1991.

[11] L. F. Henderson. *On the fluid mechanics of human crowd motion.* Transportation research, 8(6):509-515, 1974.

[12] S. Hoogendoorn and P. H. L. Bovy. *Simulation of pedestrian flows by optimal control and differential games.* Optimal Control Applications and Methods 24(3): 153-172, 2003.

[13] M. Huber, Y. H. Su, M. Krüger, K. Faschian, S. Glasauer and J. Hermsdörfer. *Adjustments of speed and path when avoiding collisions with another pedestrian.* PloS one, 9(2), e89589, 2014.

[14] A. Lachapelle and M–T. Wolfram. *On a mean field game approach modeling congestion and aversion in pedestrian crowds.* Transportation research part B: methodological 45(10):1572-1589, 2011.

[15] A. J. Mayne. *Some further results in the theory of pedestrians and road traffic.* Biometrika, 41(3-4):375-389, 1954.

[16] G. Naldi, L. Pareschi, and G. Toscani. eds. *Mathematical modeling of collective behavior in socio-economic and life sciences.* Springer Science & Business Media, 2010.

[17] P. Neittaanmaki and D. Tiba. Optimal Control of Nonlinear Parabolic Systems: Theory, Algorithms and Applications. *Pure and Applied Mathematics, CRC Press*, 1994.

[18] A. H. Olivier, A. Marin, A. Crétual and J. Pettré. *Minimal predicted distance: A common metric for collision avoidance during pairwise interactions between walkers.* Gait & posture, 36(3):399-404, 2012.

[19] B. Piccoli and A. Tosin. *Time-evolving measures and macroscopic modeling of pedestrian flow.* Archive for Rational Mechanics and Analysis 199(3):707-738, 2011.

[20] S. Roy, M. Annunziato and A. Borzì. *A Fokker-Planck Feedback Control-Constrained Approach for modeling Crowd Motion.* Journal of Computational and Theoretical Transport, 45(6):442-458, 2016.

[21] F. Tröltzsch. *Optimal Control of Partial Differential Equations*, AMS, Providence, RI, 2010.

[22] A. Turnwald, D. Althoff, D. Wollherr and M. Buss. *Understanding human avoidance behavior: interaction-aware decision making based on game theory.* International Journal of Social Robotics, 8(2):331-351, 2016.